Desalination and Water Treatment
www.deswater.com
doi: 10.5004/dwt.2022.29092

280 (2022) 271–281
December

A green synthesis of Fe_3O_4 nanocomposites loaded castor seed shell carbon for lead(II) removal from water: equilibrium and kinetic studies

Rasappan Vaithianathan[a,*], Panneerselvam Anitha[a], Arumugam Ramachandran[a], Ramasamy Sudha[b]

[a]*Centre for Research, Department of Chemistry, Government College of Engineering, Salem-636 011, Tamil Nadu, India, emails: rvnkishan@gmail.com (R. Vaithianathan), anitha1180@gmail.com (P. Anitha), rams.anbu@gmail.com (A. Ramachandran)*
[b]*Departent of Chemistry, Vivekanandha College of Arts and Sciences for Women, Tiruchengode-637 205, Tamil Nadu, India, email: drsudha@vicas.org (R. Sudha)*

Received 13 June 2022; Accepted 25 October 2022

ABSTRACT

The adsorption performance of Pb(II) ions from an aqueous solution was successfully tested by magnetic nanocomposites loaded with activated carbon. The activated carbon is prepared from castor seed shells used as an adsorbent (MCSSC) by co-precipitation and thermal activation. The prepared MCSSC is compared with raw castor seed shell (CSS) under batch experiments such as optimum contact time for various concentrations, pH, adsorbent dose and temperature. Fourier-transform infrared spectroscopy, scanning electron microscopy and energy-dispersive X-ray spectroscopy analysis explored the functionality, surface morphology and elemental composition of MCSSC and CSS. The data of equilibrium was found to fit well with the Langmuir model, confirming that the monolayer coating of Pb(II) ion onto MCSSC and CSS was 350.45 and 25.75 mg g^{-1}, respectively. Following the kinetic data, a pseudo-second-order model with a film diffusion mechanism was developed. According to thermodynamic studies, the uptake of lead(II) ions was shown to be spontaneous and exothermic. The Langmuir adsorption isotherm equation was used to create a single-stage batch adsorber. Compared to CSS, the regeneration study revealed that MCSSC could successfully remove Pb(II) ions for five operation cycles.

Keywords: Lead(II); Isotherm; Castor seed shell; Thermodynamics

1. Introduction

Researchers from all across the globe are focusing their attention on a potentially catastrophic environmental issue known as water pollution. The fast growth of both industry and population are the root causes of this issue since both of these factors lead to the degradation of water supplies. The direct disposal of untreated sanitary waste, toxic industrial effluents and runoff from agricultural fields into water resources like rivers, lakes, ponds and wells are the primary causes. Most of the world's population encounters the problem of clean drinking water, and conditions are adverse in developing countries [1]. Lead is one of the toxic heavy metals and has been broadly used in the modern industry for product manufacture. Lead can transfer from soils to plants and animals and then is exposed to human beings through the food chain. Lead levels in drinking water and surface water intended for drinking are regulated at 0.010 and 0.015 mg L^{-1}, respectively by the EU, WHO and USEPA [2]. Therefore, it is essential to develop effective technologies to treat lead polluted wastewater before its discharge into the natural environment.

* Corresponding author.

Various technologies have been developed to remove lead(II) ions from an aqueous solution, such as ion exchange, membrane process, chemical precipitation, electrochemical treatment, and reverse osmosis. However, these technologies are sometimes restricted due to technical or economic constraints [3]. Nowadays, researchers have focused on new technology like adsorption, one of the most promising approaches for removing metallic containment from wastewater.

Many scientists have reported a low cost and high efficiency of adsorbents prepared from several basic and chemically modified natural wastes. The agricultural wastes such as palm oil solid waste [4], red mud [5], *Cassia fistula* seeds [6], tamarind seed [7] and *Bauhinia variegata* leaves [8] have been successfully applied for the elimination of lead(II) ions from aqueous solution. However, separating the adsorbents from wastewater is difficult due to their incomplete precipitation. Hence, scientists have explored a magnetic nanoparticle-loaded activated carbon as a suitable method to separate solid particles from the suspension by applying an external magnetic field. This technique has recently gained eminence in the water treatment process and is now recognized as a prospective technique for resolving the above-mentioned issues. However, little work has been done on the preparation of magnetic nanoparticle loaded agricultural waste activated carbon such as litchi peel [3], corncob [9], pomegranate peel [10] and *Bauhinia purpurea* pods [11] are used as adsorbents directly on the application to the removal of heavy metal ions from aqueous solution.

This study aimed to construct a new magnetic adsorbent (MCSSC) using Fe_3O_4 magnetic nanoparticles loaded carbon generated from castor seed shell and compare it to raw castor seed shell for the removal of Pb(II) ions from bulk solution and wastewater. Fourier-transform infrared spectroscopy (FTIR), scanning electron microscopy (SEM), and energy-dispersive X-ray spectroscopy (EDX) characterize the magnetic adsorbents produced. The maximum lead(II) removal ability of MCSSC was optimized by various factors of contact time, pH, adsorbent dose and temperature using a batch experiment. The adsorption isotherms, kinetics and thermodynamic parameters for the adsorption of Pb(II) ions on MCSSC are also determined to estimate the adsorption process. The suitability of the prepared MCSSC was checked by collecting the wastewater sample from the nearby industrial area in Tiruppur.

2. Materials and methods

2.1. Preparation of the Pb(II) solutions

1.59 g of $Pb(NO_3)_2$ was dissolved in 1,000 mL of distilled water to make an aqueous solution of 1,000 mg L^{-1} of Pb(II) as stock. Dilution of the stock solution yielded lead(II) solutions with the desired concentrations of 10–60 mg L^{-1} and stored in air tight container. In addition, 0.1 N HCl or 0.1 N NaOH solutions were used to alter the pH of the solution to neutral. The lead-plating industry wastewater was collected from M/S metal platers in Tiruppur, India. Because the wastewater has a very high concentration of lead (1,010 mg L^{-1}), it was diluted to 10 times for the studies with CSS and MCSSC.

2.2. Synthesis of raw castor seed shell

Castor seed shell was collected from the local area in Salem district, Tamil Nadu, India. The collected raw material was washed carefully with deionised water to remove dust particles and other impurities. The collected raw materials were dried in a hot air oven at 100°C for 4 h, crushed into powder, and stored in a bottle.

2.3. Synthesis of magnetic castor seed shell-based carbon

About 10 g of anhydrous ferric chloride ($FeCl_3$) and 5 g of ferrous chloride ($FeCl_2{\cdot}6H_2O$) was mixed in 200 mL of distilled water and stirred vigorously at 80°C for 30 min. Then 12 g of powered castor seed shell was added, and the solution was stirred for 1 h. Then 20 mL of 25% NaOH solution was added drop wise, and stirring was continued until the black–coloured precipitate was obtained. The precipitate was filtered and dried at 100°C for 12 h. The resultant impregnated samples were activated at 450°C for 3 h in a muffle furnace. After cooling, the activated sample was rinsed with deionized water until the filtrate pH was about 6–7 and dried in a hot air oven for 6 h at 110°C. The obtained samples were named magnetic castor seed shell-based carbon (MCSSC) and stored in a bottle for further experiments.

2.4. Characterisation of MCSSC

SEM at an accelerating voltage of 15 kV with EDX and (FTIR, SHIMADZU, Japan, Spectrometer of wave number range 400–4,000 cm^{-1}) was used to characterise the prepared magnetic castor seed shell-based carbon (MCSSC).

2.5. Batch adsorption studies

Batch adsorption studies have been carried out in plastic bottles of 300 mL capacity containing 100 mL of 10 mg L^{-1} initial lead(II) concentration and 0.1 g of adsorbent at pH 7.0. Then the reaction mixture was shaken in a temperature-controlled shaker at a constant speed of 200 rpm at room temperature to change the time for various intervals. The influence of solution pH was identified by adjusting the pH to a specific value using 0.1 N of HCl/NaOH solutions. The isotherm study was performed with variations in the initial concentration of Pb(II), such as 10–60 mg L^{-1} at 27°C, 37°C, and 47°C. The kinetic studies were conducted for various Pb(II) concentrations over the range of 5, 7, and 10 mg L^{-1} at an optimum pH and room temperature. Each test was repeated three times, and the work reported consistent values.

The contents were centrifuged, filtered, and the concentration level of Pb(II) was determined using an atomic absorption spectrophotometer (ELICO Model-SL 163, India) at the end of the equilibrium time. Eqs. (1) and (2) were used to calculate the percentage removal of lead(II) and the adsorption capacity [11].

$$\%\ \text{Removal of lead} = \frac{C_0 - C_e}{C_0} \times 100 \quad (1)$$

$$\text{Adsorption capacity}\left(q_e\right)=\frac{C_0-C_e}{M}\times V \tag{2}$$

where C_0 and C_e are the Pb(II) concentrations in mg L^{-1} at initial and equilibrium, respectively; M is the adsorbent's mass in g; V is the Pb(II) solution's volume in L; q_e is the adsorption capacity at equilibrium (mg g^{-1}).

2.6. Adsorption isotherms

Adsorption isotherms are essential for the development of any adsorption process. At equilibrium, the chemical potential of the solute in the solid phase is identical to that in the liquid phase. The adsorption of lead(II) ions at equilibrium onto CSS and MCSSC were correlated by applying the non-linear forms of four different isotherm equations such as Freundlich [12], Langmuir [13], Temkin [14] and Dubinin–Radushkevich [15] at different temperatures (27°C–47°C) using MATLAB R2010b.

The Freundlich adsorption isotherm is a commonly used empirical equation applicable to assume the formation of a multilayer of adsorbates on the adsorbent's surface.

$$q_e=K_F C_e^{1/n} \tag{3}$$

where n (g L^{-1}) is the degree of non-linearity between adsorption and solution concentration and K_F is the Freundlich bonding energy constant (mg g^{-1})(L $mg^{-1})^{(1/n)}$). If $n > 1$, adsorption is a physical process; if $n = 1$ is linear; if $n < 1$ is a chemical process.

The Langmuir adsorption isotherm model is based on monolayer adsorption onto a homogeneous structure without any reaction between the adsorbed molecules and is represented as follows:

$$q_e=\frac{q_m K_L C_e}{1+K_L C_e} \tag{4}$$

The maximum monolayer adsorption capacity is q_m (mg g^{-1}), while the Langmuir constant 'K_L' (L mg^{-1}) corresponding to adsorption energy. The dimensionless equilibrium parameter, "R_L" can be used to measure the attraction between the sorbent and the sorbate by expressing the main properties of the Langmuir isotherm parameters as follows [16]:

$$R_L=\frac{1}{1+K_L C_0} \tag{5}$$

where C_0 is the initial Pb(II) ion concentration and K_L is the Langmuir sorption constant. When the value of R_L is between 0 and 1, adsorption is advantageous. The isotherm is classified as irreversible ($R_L = 0$), favourable ($0 < R_L < 1$), linear ($R_L = 1$), or unfavourable ($R_L > 1$) based on the value of R_L.

The Temkin isotherm presumes a linear decline rather than a logarithmic drop in the heat of adsorption while ignoring extremely low and extremely high concentrations and is given as:

$$q_e=B\ln\left(AC_e\right) \tag{6}$$

where B is a constant related to the heat of adsorption (kJ mol^{-1}) and A (L mg^{-1}) is the equilibrium binding constant related to the maximum binding energy.

Dubinin–Radushkevich model presumes that the adsorbent's surface is heterogeneous and used to fix the type of adsorption process and expressed mathematically by the Eq. (7):

$$q_e=q_{mD}e^{-\beta\varepsilon^2} \tag{7}$$

where q_{mD} is the Dubinin–Radushkevich monolayer capacity in (mg g^{-1}), β is sorption energy constant, and the Polanyi potential 'ε', is given as:

$$\varepsilon=RT\ln\left[1+\frac{1}{C_e}\right] \tag{8}$$

where T is the absolute temperature, while R is the gas constant (8.314 J mol^{-1} K^{-1}). The constant β is the activity coefficient, which may be used to compute the mean adsorption free energy E:

$$E=\left[\frac{1}{\sqrt{2\beta}}\right] \tag{9}$$

The value of E tells us a lot about the type of adsorption mechanism. If the E value is less than 8 kJ mol^{-1}, the adsorption is considered physical. If the E is between 8–16 kJ mol^{-1}, the adsorption is either ion-exchange or chemical [17].

2.7. Thermodynamic and kinetic studies

0.1 g for MCSSC and an adsorbent dose of 0.3 g for CSS were added to 100 mL of 10 mg L^{-1} of lead(II) solution at pH 6.0, and the impact of temperature around 27°C–47°C on lead(II) adsorption onto CSS and MCSSC was investigated. The various thermodynamic parameters such as $\Delta G°$, $\Delta H°$, and $\Delta S°$ were estimated from the experimental data using the Van't Hoff equation is expressed as follows [18]:

$$\ln K_c=\frac{\Delta G°}{RT}=\frac{\Delta S°}{R}-\frac{\Delta H°}{RT} \tag{10}$$

where K_c is the thermodynamic equilibrium constant that can be calculated by the following equation [19]:

$$K_c=\frac{q_e}{C_e} \tag{11}$$

where q_e and C_e (mg L^{-1}) are the equilibrium adsorption capacities and concentration of Pb(II) ions. The $\Delta S°$ and $\Delta H°$ values estimated from the intercept and slope of a plot of $\ln K_c$ vs. $1/T$, respectively. The values of $\Delta G°$ at different temperatures were calculated from Eq. (12):

$$\Delta G^\circ = -RT\ln K_c \tag{12}$$

The adsorption kinetics mainly studies the specific process and rate of adsorption of adsorbate on the adsorbent, and the specific adsorption process and rate directly affect the adsorption effect. Therefore, studying adsorption kinetics helps understand the adsorption reaction's mechanism and predict pollutants migration and fate behaviour.

Lagergren's pseudo-first-order reaction equation [20] was frequently utilised for liquid/solid system adsorption based on solid capacity. Eq. (13) is the relation between the adsorption amounts at time t (min), q_t (mg g^{-1}), and at equilibrium, q_e (mg g^{-1}) with the rate constant, k_1 (min^{-1}) for the pseudo-first-order adsorption.

$$\log\left(q_e - q_t\right) = \log q_e - \frac{k_1}{2.303}t \tag{13}$$

A pseudo-second-order model that assumes adsorption follows second-order rate equations [21]. The linear form of the model is shown as follows:

$$\frac{t}{q_t} = \frac{1}{k_2 q_e^2} + \frac{t}{q_e} \tag{14}$$

where k_2 (g mg^{-1} min^{-1}) is the adsorption rate constant. The rate of adsorption at the initial stage 'h_0' (mg g^{-1} min^{-1}) is given as [22]:

$$h_0 = k_2 q_e^2 \tag{15}$$

3. Results and discussion

3.1. Fourier-transform infrared spectroscopy studies

FTIR spectroscopy is an essential tool for the identification of functional group's present on the adsorbent surface. The FTIR spectrum of magnetic adsorbents before Fig. 1a and b and after the adsorption Pb(II) are shown in Fig. 1c and d. The presence of the Fe–O group is observed in MCSSC around 570 cm^{-1} [23]. The peak at the O–H stretching vibrations ranges from 3,417 cm^{-1} of CSS, has shift to 3,448 cm^{-1} in MCSSC which is responsible for the metal-binding process and further shift during lead adsorption [24–26]. The C=O stretching of the –COOH group, represented by the band around 1,637; 1,641; 1,645 and 1,651 cm^{-1} for CSS, MCSSC, Pb-CSS and Pb-MCSSC respectively [27]. Similarly, for the aromatic C=C ring band appeared at 1,530; 1,548; 1,544 and 1,558 cm^{-1} [28]. The FTIR spectrum of lead(II) ions loaded CSS and MCSSC indicated that the peak values are changed slightly from the original position and their intensity is shifted. The above observation showed that hydroxyl and carboxylic acid groups in CSS and in addition to that Fe–O groups conformed in MCSSC, which is responsible for the adsorption of Pb(II) ions from the aqueous solution.

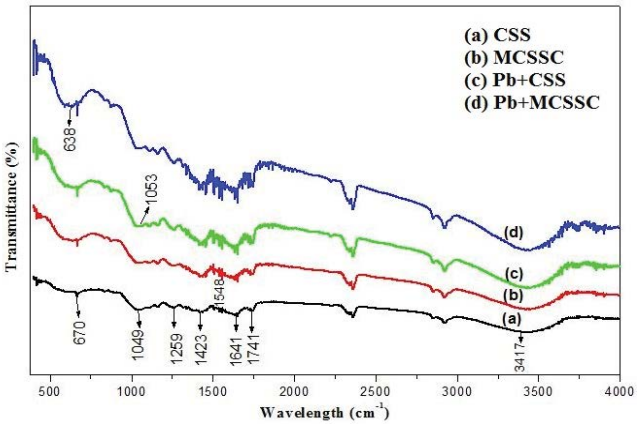

Fig. 1. FTIR spectra of (a) CSS, (b) MCSSC, (c) Pb + CSS and (d) Pb + MCSSC.

3.2. SEM and EDX studies

Fig. 2a and b show SEM images of CSS and MCSSC adsorbents, which reveal a microporous structure visible in the fissures and holes. EDX study confirms the adsorption of metal ions as seen by SEM image of the CSS and MCSSC before and after adsorption. The pores on CSS and MCSSC are covered after the metal ions have been absorbed. The EDX spectra showed that the adsorption of Pb(II) ion in addition to that other cation in CSS and MCSSC. The peak of spectra supporting the Pb(II) ions adsorption on the CSS and MCSSC surface (Fig. 2c and d).

3.3. Effect of agitation time and initial metal ion concentration

Agitation time is an important parameter affecting toxic metal ions on the adsorption rate [29]. The removal of lead(II) ions was calculated as a function of agitation time and initial concentrations at varying agitation time (30–180 min) and initial lead(II) concentrations (10–30 mg L^{-1}) using pH 7.0 and constant adsorbent dose of 0.1 g L^{-1}. Fig. 3a and b show that the sorption efficiency increases rapidly with time and attains equilibrium for 120 min for CSS and MCSSC. Further increase in the agitation time does not affect the removal process; that may be due to exhaustion of binding sites in CSS and MCSSC. Hence, the optimal contact time was found to be 120 min and maintained for further experiments. The lead(II) removal capacity is decreased with increasing initial lead(II) concentrations. At higher concentrations, the availability of lead(II) ions is higher, which in turn might provide a higher driving force for the metal ions from the solution to the sorbents.

3.4. pH effect

The pH of the solution is a crucial factor that determines the adsorption performance of the adsorbent [30]. The effect of pH was investigated by adjusting the initial pH from 2.0–10.0 on the removal of 100 mL of 10 mg L^{-1} lead(II) ions by CSS and MCSSC, whereas all other parameters was taken a constant value. In aqueous solutions, metal species exist as Pb^{2+}, $Pb(OH)^+$, and $Pb(OH)_2$ and at pH below 5.0, $Pb(OH)_2$ is soluble, hence Pb^{2+} is the dominant species

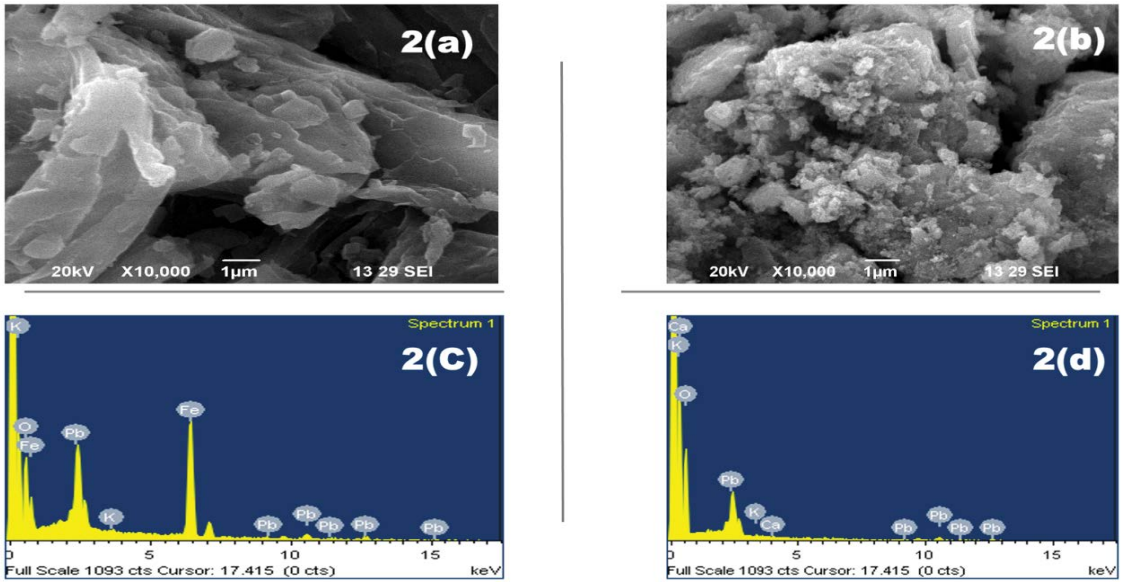

Fig. 2. SEM and EDX image of (a) CSS, (b) MCSSC, (c) Pb + CSS and (d) Pb + MCSSC.

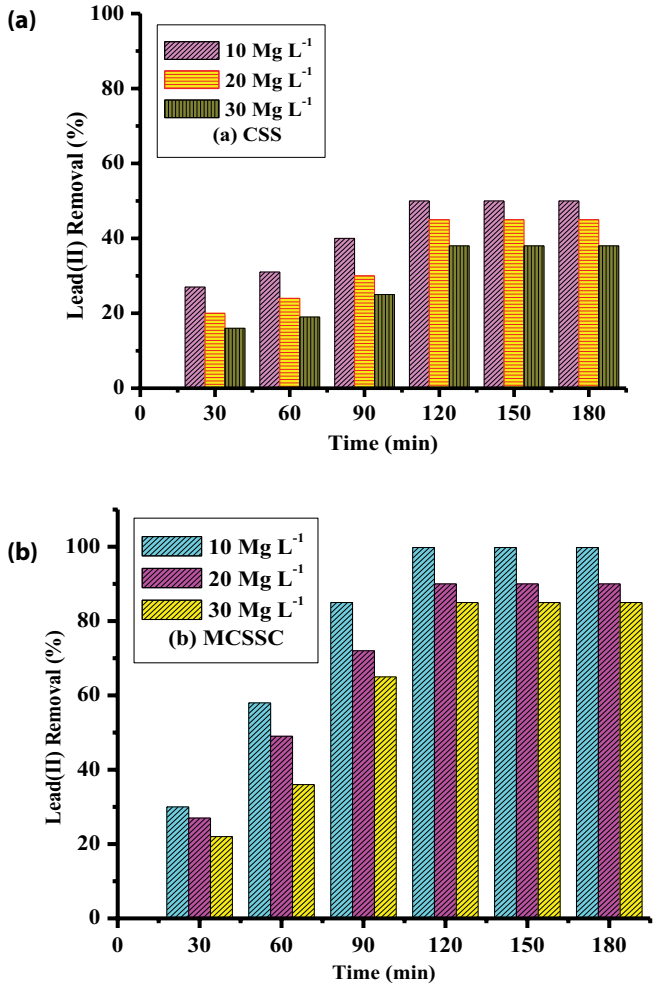

Fig. 3. (a,b) Effect of agitation time for the removal of lead(II) onto CSS and MCSSC.

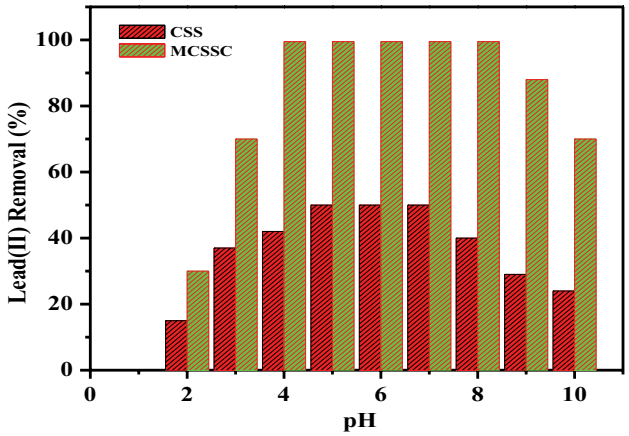

Fig. 4. Effect of pH for the removal of lead(II) onto CSS and MCSSC.

in solution. At pH 10.0, $Pb(OH)_2$ solubility is quite low and here, hydroxide traces dominate the solution. In alkaline range, $Pb(OH)_2$ production and precipitation remove Pb^{2+} ions. Since the objective was to remove metal ions by adsorption rather than precipitation, all studies were conducted at a maximum starting solution pH of 4.0, with the variation increasing with initial metal ion concentration [31].

Fig. 4 clearly shows that the percentage removal of lead(II) increased with increasing pH and attained the maximum percentage removal of 50% ± (0.4)% and 99% ± (0.5)% for CSS and MCSSC at pH 5.0–7.0 and 4.0–8.0 respectively. At low pH values, the uptake of Pb^{2+} is decreased because the adsorbent surface may be converted into highly protonated due to the presence of H^+ ions which started opposite with positively charged cationic lead(II) ions for the adsorption sites. The possible sorption mechanism that may take place at different pH conditions is represented as follows:

$$MCSSC-OH \leftrightarrow MCSSC-O^- + H^+$$

$$MCSSC-O^- + Pb^{2+} \leftrightarrow MCSSC-O-Pb$$

At higher pH, the adsorbent's surface acquires a negative charge due to surface functional group dissociation and thereby causing repulsions to the negatively charged adsorbate species, namely $Pb(OH)_3^{1-}$ and $Pb(OH)_4^{2-}$ and hence, the removal of lead(II) is not as much of favoured. In the intermediate pH, it was found that the number of H^+ ions is decreased, and the surface of magnetic castor seed shell-based activated carbon (MCSSC) becomes negatively charged and favours the sorption of positively charged metal ions due to attraction between electrostatics [32,33].

3.5. Effect of adsorbent dose

The adsorbent dose is a vital parameter for determining the adsorbent's adsorption capacity for removing polluted ions from the wastewater. In the present research, the adsorbent dose was varied from 0.05 to 0.35 g in 100 mL of 10 mg L^{-1} lead(II) solutions, while all the other optimum variables such as contact time of 120 min and at pH 6.0. Fig. 5 shows that the percentage of lead(II) extraction is increased from 30% ± 0.5% to 65% ± 0.4% with CSS dose and 75% ± 0.4% to 99.5% ± 0.5% with MCSSC. After that, it remains constant for both the adsorbents. It reveals that as the adsorbent dose increases, the number of active sites of the adsorbent also increases. After an optimum dose, a steady state is reached with an almost insignificant increase in lead(II) removal, which may be due to the adsorption site aggregation or overlapping with the increase in adsorbent dose [34].

3.6. Adsorption isotherms

The isotherm constants, correlation coefficients (R^2), sum of squares error (SSE) and root mean squared error (RMSE) values for the adsorption of lead(II) ions were estimated from the plot of non-linear isotherm curve q_e vs. C_e (Fig. 6a and b) and are listed in Table 1. The R^2 values closer to 1 and small SSE, RMSE values indicate better curve fitting. The results of table shows that the better fitting of the data by the Langmuir model compared with the other three isotherm models based on the greater R^2 and small SSE, RMSE values. This finding supports the presence of a homogenous monolayer of lead(II) ions on CSS and MCSSC. Pb(II) ions had a maximum monolayer adsorption capacity of 350.45 mg g^{-1} on MCSSC, which was 13.6 times larger than CSS (25.75 mg g^{-1}). The Langmuir isotherm's R_L values range from 0 to 1, suggesting that Pb(II) ions adsorb well onto CSS and MCSSC. From this study, the uptake of Pb(II) ions onto CSS and MCSSC from an aqueous solution is decreased with increasing temperature indicating that the adsorption process is exothermic. The calculated E values

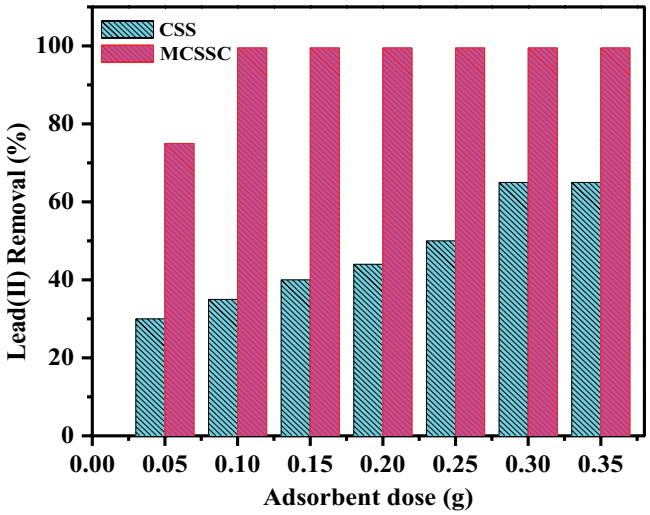

Fig. 5. Effect of adsorbent dose for the removal of lead(II) onto CSS and MCSSC.

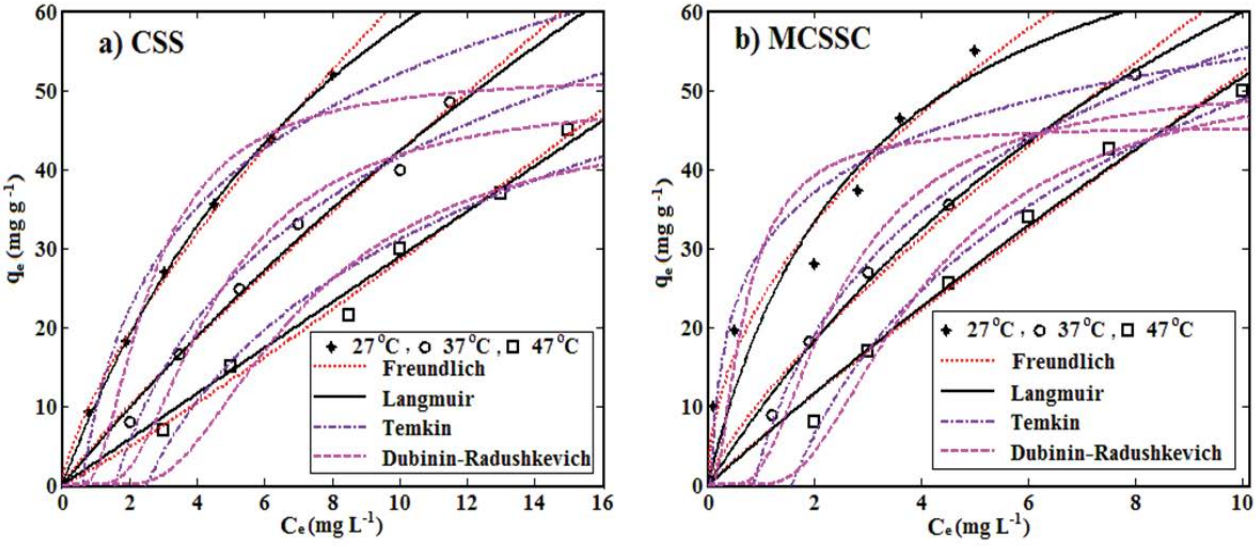

Fig. 6. Non-linear adsorption isotherms for Pb(II) with (a) CSS and (b) MCSSC.

Table 1
Non-linear isotherm and thermodynamic parameters for Pb(II) removal from aqueous solutions

Isotherm models and thermodynamics	Parameters	Temperature (K)					
		CSS			MCSSC		
		27°C	37°C	47°C	27°C	37°C	47°C
Freundlich	K_F (mg g^{-1})	5.034	4.923	3.727	9.934	8.497	6.450
	n (g L^{-1})	2.595	2.605	2.334	2.531	2.187	1.724
	SSE	4.508	3.680	3.483	18.11	15.78	13.89
	RMSE	1.062	0.819	1.060	1.085	1.095	1.055
	R^2	0.965	0.964	0.940	0.953	0.943	0.941
Langmuir	q_m (mg g^{-1})	25.75	20.45	15.75	350.45	310.85	285.35
	b (L mg^{-1})	0.137	0.102	0.080	0.188	0.132	0.110
	SSE	2.021	2.012	1.136	13.08	3.279	1.056
	RMSE	0.710	0.690	0.533	1.015	1.039	0.476
	R^2	0.995	0.998	0.997	0.998	0.998	0.997
	R_L	0.422–0.109	0.495–0.140	0.556–0.172	0.746–0.329	0.746–0.329	0.741–0.323
Temkin	A (L mg^{-1})	1.476	1.004	0.552	2.116	0.775	0.379
	B	2.420	1.863	1.890	3.482	3.542	3.727
	b (kJ mol^{-1})	1.037	1.383	1.408	0.716	0.728	0.714
	SSE	3.858	2.649	1.770	15.57	10.44	6.924
	RMSE	0.972	0.814	0.786	1.987	1.615	1.316
	R^2	0.965	0.965	0.969	0.965	0.965	0.968
Dubinin–Radushkevich	q_{mD} (mg g^{-1})	19.68	14.56	13.02	28.32	24.15	20.76
	$\beta \times 10^{-7}$ ((mol K kJ^{-1})^2)	3.265	6.479	7.436	1.854	2.312	2.688
	E (kJ mol^{-1})	1.238	0.878	0.819	1.642	1.471	1.370
	SSE	13.39	14.23	13.28	45.55	39.53	20.75
	RMSE	1.889	1.886	0.907	2.887	3.144	1.277
	R^2	0.792	0.810	0.945	0.773	0.856	0.901
Thermodynamic	$\Delta G°$ (kJ mol^{-1})	–4.340	–3.583	–2.740	–15.48	–7.577	–5.560
	$\Delta H°$ (kJ mol^{-1})	–28.268			–171.268		
	$\Delta S°$ (kJ mol^{-1} K^{-1})	–0.517			–0.517		

of the present study is below 8 kJ mol^{-1}, which indicates that the adsorption of Pb(II) ions onto the CSS and MCSSC follows physical adsorption type. Therefore, the adsorption of Pb(II) ions onto MCSSC surface is a complex, involving more than one mechanism.

The adsorptions capacities of CSS and MCSSC towards Pb^{2+} have been compared with various adsorbents reported in the literature and are listed in Table 2. Therefore, it is reasonable to infer that MCSSC has a promising adsorbent for removing Pb(II) ions from aqueous solutions because its monolayer adsorption capacity is equivalent to that of other researchers.

3.7. Thermodynamic studies and kinetic adsorption studies of CSS and MCSSC

As shown in Table 1, the negative $\Delta G°$ values inferred the adsorption of Pb(II) ions on CSS and MCSSC is spontaneous. However, the negative value of $\Delta H°$ suggests that the adsorption process is exothermic.The $\Delta G°$ value is more negative when decreasing the temperature, suggesting that lower temperatures favor the adsorption. The negative $\Delta H°$ value indicates the exothermic nature of adsorption

Table 2
Comparison of monolayer adsorption capacities in the literature for Pb(II) adsorption onto CSS and MCSSC

Adsorbents	Adsorption capacity, q_m (mg g^{-1})	References
Litchi peels	78.74	[8]
Corncob nanocomposite	11.00	[3]
Mango peel	38.31	[35]
Wine making waste	38.00	[36]
Sugarcane bagasse	19.30	[37]
Oyster shells	0.80	[38]
Sugarcane bagasse	1.61	[39]
Citrus limon (lemon) peel extract	9.01	[40]
Green coconut shell	54.62	[41]
Tagua shell	22.03	[42]
Teff straw	94.35	[43]
CSS	25.75	Present study
MCSSC	350.45	Present study

and the $\Delta S°$ can be used to describe the randomness at the adsorbent-solution interface during the sorption.

The values of k_1, R^2 and q_e at various concentrations were computed using linear plots of log (q_e–q_t) vs. t, as shown in Table 3. The pseudo-first-order kinetic model's correlation coefficients (R^2) were low. Moreover, there was a significant divergence between the experimental and estimated equilibrium adsorption capacity (q_e), showing that the Pb(II) ions adsorption on both adsorbents does not follow the pseudo-first-order kinetic model.

If pseudo-second-order kinetics is applicable, the plot of t/q_t vs. t should provide a straight line, and the slope and intercept of the plot can be used to derive q_e, k_2, and h. At all initial Pb(II) concentrations, the straight lines with R^2 value near 1 were observed and shown in Table 3. In addition, the estimated values of q_e are similar to the experimental values of q_e, which means that the second-order kinetics well represents adsorption data and that the rate-determining step of Pb(II) ions in CSS and MCSSC can be chemisorption. The rate constant k_2 values decreased with the initial Pb(II) concentration of CSS and MCSSC. The above behaviour can be attributed to the small competition of over sorption sites in low concentrations. In higher concentrations, competition for the active site will be higher, resulting in lower rates of sorption.

3.8. Mechanism of adsorption

The mechanism of diffusion and rate-determining slow step was not explained by the Lagergren's, Ho and McKay kinetic models for the adsorption of Pb(II) ions on the CSS and MCSSC. The intraparticle diffusion model explains it. Solute transfer in a solid–liquid sorption process is characterised by intraparticle diffusion, external mass transfer, or both. The following three processes were involved in the adsorption of Pb(II) ions onto CSS and MCSSC [44]:

- The migration of adsorbate molecules to the adsorbent particles' interior (intraparticle diffusion).
- Adsorbate molecules are migrated to the adsorbent's exterior surface from a bulk solution (film diffusion).
- The surface of the pores and capillary gaps are filled by an adsorbent solute (sorption).

Weber and Morris's intraparticle diffusion model [45] was used to understand the diffusion mechanism to analyse the effects of contact time data.

$$q_t = k_d t^{1/2} + I \tag{16}$$

where k_d is the intraparticle diffusion rate constant (mg g^{-1} min$^{1/2}$). From the linear plots of q_t vs. $t_{1/2}$ shown in Fig. 7a and b, the intercept I (mg g^{-1}) and the slope 'k_d' are measured. Due to the changing level of adsorption in the start and final stages of the adsorption experiment, the curve has a dual nature. The early-stage sorption can explain this was occurred by boundary layer diffusion, whilst the intraparticle diffusion was observed in the later stages (a linear portion of the curve). The boundary layer effect is reflected in the plot's intercept. The larger the intercept, the more the surface sorption will contribute to the rate-controlling step. Intraparticle diffusion is the sole rate-limiting phase if the linear lines of the plot of q_t vs. $t^{1/2}$ pass through the origin. In this study, the non-linear lines, which are not passed through the origin, imply that intraparticle diffusion was the rate-limiting of adsorption and the boundary layer effect was the rate-controlling step or both occurred simultaneously.

Table 3
Kinetic parameters for the adsorption of Pb(II) ions onto CSS and MCSSC at different initial concentrations

Kinetic model	Parameters	Concentrations (mg L^{-1})					
		CSS			MCSSC		
		5	7	10	5	7	10
Pseudo-first-order	$q_{e,exp}$ (mg g^{-1})	4.79	6.76	9.30	4.93	6.93	9.98
	k_1 (min^{-1})	0.014	0.012	0.021	0.016	0.012	0.018
	$q_{e,cal}$ (mg g^{-1})	2.30	3.08	4.74	1.25	2.06	3.36
	R^2	0.878	0.898	0.914	0.980	0.971	0.960
	P %	51.98	54.44	49.03	74.65	70.27	66.33
Pseudo-second-order	k_2 (g mg^{-1} min^{-1})	0.010	0.009	0.006	0.030	0.020	0.010
	$q_{e,cal}$ (mg g^{-1})	4.98	6.99	9.50	5.03	7.25	10.42
	h_0 (mg g^{-1} min^{-1})	0.229	0.411	0.519	0.729	0.960	0.996
	R^2	0.999	0.999	0.999	0.999	0.999	0.999
	P %	3.97	3.40	2.15	2.03	4.62	4.41
Intraparticle diffusion	k_d (mg g^{-1} min$^{-1/2)}$	0.107	0.131	0.142	0.046	0.140	0.166
	I (mg g^{-1})	2.927	4.422	6.852	4.065	4.604	7.390
	R^2	0.857	0.938	0.884	0.753	0.733	0.854
Film diffusion	D_f (×10^{-8} cm^2 s^{-1})	0.550	0.670	0.615	1.658	1.528	1.100
Pore diffusion	D_p (×10^{-8} cm^2 s^{-1})	2.149	2.589	2.480	6.282	5.786	4.133

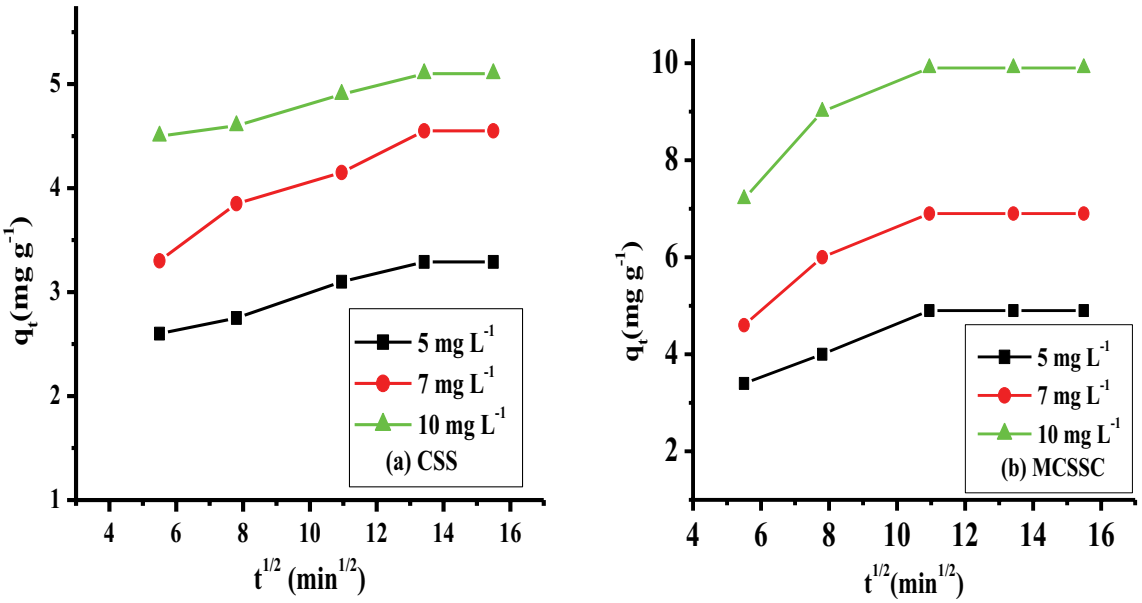

Fig. 7. Intraparticle diffusion model for the adsorption of Pb(II) ions onto (a) CSS and (b) MCSSC.

The film and pore diffusion coefficients for different Pb(II) ions concentrations were computed using the following equations [46].

$$D_f = \frac{0.23 r_o d t_{1/2} C^*}{C} \quad (17)$$

$$D_p = \frac{0.03 r_o^2}{t_{1/2}} \quad (18)$$

where D_f is the diffusion coefficient for the film (cm^2 s^{-1}), D_p is the diffusion coefficient for pore (cm^2 s^{-1}), r_o is the sorbent' radius (cm), and $t_{1/2}$ is the half-life period (s), d is the film's thickness in cm, and C^*/C is sorbent's loading at equilibrium.

If the film diffusion coefficient (D_f) values between 10^{-6}–10^{-8} cm^2 s^{-1}, then the film diffusion is the key mechanism of the rate-determining step in the adsorption of the heavy metals on a sorbent [47]. If pore diffusion D_p is to be used as a rate-determining mechanism, it should have a value range of 10^{-11}–10^{-13} cm^2 s^{-1}. For this investigation, the film and pore diffusion coefficients were calculated from the pseudo-second-order rate constant (k_2). Table 3 shows that the D_f value is closer to 10^{-6}–10^{-8} cm^2 s^{-1} infers a film diffusion process during the removal of Pb(II) ions.

3.9. Design of batch adsorption experiments

The best fit of the Langmuir isotherm model equation is utilised [48] to estimate the single-stage pattern of batch adsorber system. The experimental aim is to decline the initial Pb(II) ions amount in the volume of solution V (L) from C_0 to C_e (mg L^{-1}). The amount of MCSSC adsorbent is M (g), and the loading of Pb(II) ions varies from q_0 to q_e (mg g^{-1}). At time t = 0, q_0 = 0 as time proceeds, the mass balance

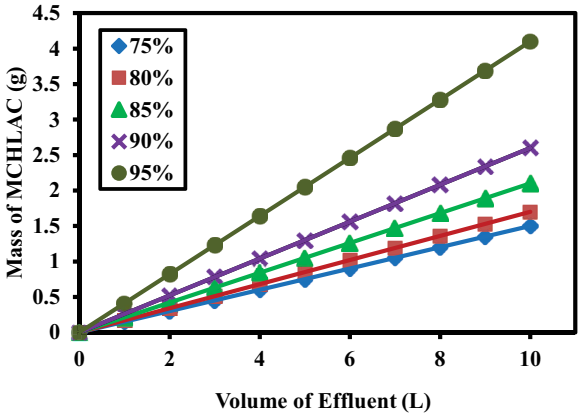

Fig. 8. Batch design plot for the adsorption of lead(II) ions onto MCSSC.

Table 4
Characteristics of lead plating industry wastewater

Parameter	Concentration
pH	1.80
Conductivity, mS cm^{-1}	13.35
Total solid, mg L^{-1}	5,580.00
Turbidity, NTU	20.00
Chloride, mg L^{-1}	650.00
Sulfate, mg L^{-1}	2,010.00
COD, mg L^{-1}	48.00
Iron, mg L^{-1}	37.50
Lead, mg L^{-1}	1,010.00
Sodium, mg L^{-1}	356.00
Calcium, mg L^{-1}	79.00
Magnesium, mg L^{-1}	158.00

Table 5
Pb(II) adsorption–desorption cycles with 0.5 mol L^{-1} HCl as regenerant

Cycles	Pb(II) C_0 (mg L^{-1})	MCSSC		CSS	
		Adsorption (%)	Recovery (%)	Adsorption (%)	Recovery (%)
1	101	99.60	99.20	44.50	44.40
2	101	99.40	99.30	32.80	31.05
3	101	99.30	98.20	26.30	23.30
4	101	99.50	99.40	20.40	19.60
5	101	99.60	99.30	13.27	12.10

equates the lead(II) ions removed from the aqueous solution to that picked by the MCSSC. The mass balance for the single-stage batch adsorption system can be expressed as:

$$V\left(C_o - C_e\right) = M\left(q_e - q_o\right) = Mq_e \tag{19}$$

$$\frac{M}{V} = \frac{C_o - C_e}{q_e} = \frac{C_o - C_e}{\frac{q_m K_L C_e}{1 + K_L C_e}} \tag{20}$$

The plot of the calculated mass of MCSSC required with an initial strength of 50 mg L^{-1} Pb(II) ions for 75%, 80%, 85%, 90% and 95% to remove Pb(II) ions at various volumes of solution (1 to 10 L) for a single-stage batch adsorption system, for which the design procedure is outlined, can be seen in Fig. 8.

4. Removal of Pb(II) from electroplating wastewater and regeneration studies

To demonstrate the usefulness of sorbents in batch mode investigations, batch experiments with lead electroplating wastewater were conducted. The characteristics of lead plating wastewater are shown in Table 4. Because of the high percentage of lead (1,010 mg L^{-1}) in wastewater was diluted 10 times before being used in CSS and MCSSC studies. A minimum MCSSC dose of 1 g L^{-1} is required to remove Pb(II) ions from wastewater containing 101 g L^{-1} of Pb(II), with maximum removal of 99% ± 0.5% for MCSSC. In the case of CSS, however, a minimum dose of 5 g L^{-1} was sufficient to produce a maximum elimination of 44% ± 0.5%. As a result of the moderate ion exchange found with MCSSC compared to CSS, MCSSC is 5 times more effective than CSS in treating lead-plating wastewater.

0.5 mol L^{-1} HCl was utilized to reproduce the adsorbent throughout five cycles of operation to examine the adsorbent's efficiency over multiple usages. The recyclability results show that the efficiency of the recycled MCSSC behaves like fresh even after five cycles of removing Pb(II) (Table 5). In the case of CSS, it was found that both adsorption and desorption decreased significantly. As a result, for the recovery of Pb(II) ions and repeated use, MCSSC is a potent adsorbent. The MCSSC and CSS showed 3.0% and 6%–7% average attrition losses, respectively, after the end of the fifth cycle during batch mode operations.

5. Conclusions

The potential of Fe_3O_4 loaded castor seed shell activated carbon was used as a cheap adsorbent for the adsorption of Pb(II) ions from bulk solution. The optimum metal ion concentrations, contact time, pH, adsorbent dose, and temperature onto MCSSC was 10 mg L^{-1}, 120 min, 6.0, 0.1 g and 27°C respectively. At 27°C, the Langmuir isotherm model fit all experimental data well, and MCSSC's maximal monolayer adsorption capacity was 350.45 mg g^{-1}, which was almost 13.6 times larger than CSS's (25.75 mg g^{-1}). The negative value of $\Delta H°$ and $\Delta G°$ indicated that the adsorption process is exothermic and spontaneous in nature and the adsorption process could be fitted by pseudo-second-order model. The MCSSC could be effectively applied for industrial wastewater and exhibited a good reusability up to five cycles as compared to that of CSS. In the view of the present research results, it could be concluded that MCSSC may be utilized as an efficient adsorbent for the removal and recovery of lead(II) ions from aqueous solution and wastewater.

References

[1] S. Ahuja, Ed., Advances in Water Purification Techniques: Meeting the Needs of Developed and Developing Countries, Elsevier, United States of America, 2018.
[2] K. Li, Z. Zheng, Y. Li, Characterization and lead adsorption properties of activated carbons prepared from cotton stalk by one-step H_3PO_4 activation, J. Hazard. Mater., 181 (2010) 440–447.
[3] R. Jiang, J. Tian, H. Zheng, J. Qi, S. Sun, X. Li, A novel magnetic adsorbent based on waste litchi peels for removing Pb(II) from aqueous solution, J. Environ. Manage., 155 (2015) 24–30.
[4] M.A. Elias, T. Hadibarata, P. Sathishkumar, Modified oil palm industry solid waste as a potential adsorbent for lead removal, Environ. Chem. Ecotoxicol., 3 (2021) 1–7.
[5] F. Lyu, S. Niu, L. Wang, R. Liu, W. Sun, D. He, Efficient removal of Pb(II) ions from aqueous solution by modified red mud, J. Hazard. Mater., 406 (2021) 124678, doi: 10.1016/j.jhazmat.2020.124678.
[6] R.V. Hemavathy, A. Saravanan, P. Senthil Kumar, D.-V.N. Vo, S. Karishma, S. Jeevanantham, Adsorptive removal of Pb(II) ions onto surface modified adsorbents derived from *Cassia fistula* seeds: optimization and modelling study, Chemosphere, 283 (2021) 131276, doi: 10.1016/j.chemosphere.2021.131276.
[7] R. Jayasree, P. Senthil Kumar, A. Saravanan, R.V. Hemavathy, P.R. Yaashikaa, P. Arthi, J. Shreshta, S. Jeevanantham, S. Karishma, M.V. Arasu, N.A. Al-Dhabi, K.C. Choi, Sequestration of toxic Pb(II) ions using ultrasonic modified agro waste: adsorption mechanism and modelling study, Chemosphere, 285 (2021) 131502, doi: 10.1016/j.chemosphere.2021.131502.
[8] S.M. Salman, M. Zahoor, A. Majeed, M. Wahab, D. Shahwar, S.N. Shah, E. Khan, Effective removal of Cd(II), Pb(II) and

Cr(VI) from aqueous solution using *Bauhinia variegata* leaves after chemical modifications, Desal. Water Treat., 220 (2021) 182–191.
[9] K.H. Kamal, M.S. Attia, N.S. Ammar, E.M. Abou-Taleb, Kinetics and isotherms of lead ions removal from wastewater using modified corncob nanocomposite, Inorg. Chem. Commun., 130 (2021) 108742, doi: 10.1016/j.inoche.2021.108742.
[10] H. Asadollahzadeh, M. Ghazizadeh, M. Manzari, Developing a magnetic nanocomposite adsorbent based on carbon quantum dots prepared from pomegranate peel for the removal of Pb(II) and Cd(II) ions from aqueous solution, Anal. Methods Environ. Chem. J., 4 (2021) 33–46.
[11] H. Çelebi, G. Gök, O. Gök, Adsorption capability of brewed tea waste in waters containing toxic lead(II), cadmium(II), nickel(II), and zinc(II) heavy metal ions, Sci. Rep., 10 (2020) 17570, doi: 10.1038/s41598-020-74553-4.
[12] H.M.F. Freundlich, Over the adsorption in solution, J. Phys. Chem., 57 (1906) 385–471.
[13] I. Langmuir, The adsorption of gases on plane surfaces of glass, mica and platinum, J. Am. Chem. Soc., 40 (1918) 1361–1403.
[14] M.J. Temkin, V. Pyzhev, Recent modifications to Langmuir isotherms, Acta Physicochim. URSS, 12 (1940) 217–225.
[15] M.M. Dubinin, L.V. Radushkevich, Equation of the characteristic curve of activated charcoal, Chem. Zentralbl., 1 (1947) 875–889.
[16] T.W. Weber, R.K. Chakravorti, Pore and solid diffusion models for fixed-bed adsorbers, AlChE J., 20 (1974) 228–238.
[17] H. Chen, G. Dai, J. Zhao, A. Zhong, J. Wu, H. Yan, Removal of copper(II) ions by a biosorbent—*Cinnamomum camphora* leaves powder, J. Hazard. Mater., 177 (2010) 228–236.
[18] S. Sun, J. Yang, Y. Li, K. Wang, X. Li, Optimizing adsorption of Pb(II) by modified litchi pericarp using the response surface methodology, Ecotoxicol. Environ. Saf., 108 (2014) 29–35.
[19] S. Liang, X.Y. Guo, N.C. Feng, Q.H. Tian, Isotherms, kinetics and thermodynamics studies of adsorption of Cu^{2+} from aqueous solutions by Mg^{2+}/K^{+} type orange peel adsorbents, J. Hazard. Mater., 174 (2010) 756–762.
[20] S. Lagergren, About the theory of so-called adsorption of solute substances, Kungliga Svenska Vetenskapsakad. Handl., 24 (1898) 1–39.
[21] Y.S. Ho, G. Mckay, Pseudo-second-order model for sorption processes, Process Biochem., 34 (1999) 451–465.
[22] Y.S. Ho, Removal of copper ions from aqueous solution by tree fern, Water Res., 37 (2003) 2323–2330.
[23] G.-y. Li, Y.-r. Jiang, K.-l. Huang, P. Ding, J. Chen, Preparation and properties of magnetic Fe_3O_4–chitosan nanoparticles, J. Alloys Compd., 466 (2008) 451–456.
[24] R. Sharma, A. Sarswat, C.U. Pittman, D. Mohan, Cadmium and lead remediation using magnetic and non-magnetic sustainable biosorbents derived from *Bauhinia purpurea* pods, RSC Adv., 7 (2017) 8606–8624.
[25] S. Sribharathi, P. Anitha, R. Sudhaa, K. Poornima, G. Kavitha, Cadmium(II) removal from aqueous solution using a novel magnetic nanoparticle impregnated onto *Citrus hystrix* leaves, Desal. Water Treat., 196 (2020) 388–401.
[26] R. Sudha, K. Srinivasan, P. Premkumar, Removal of nickel(II) from aqueous solution using *Citrus limettioides* peel and seed carbon, Ecotoxicol. Environ. Saf., 117 (2015) 115–123.
[27] R. Sudha, K. Srinivasan, Isotherm, kinetic, and thermodynamic studies on Ni(II) removal from aqueous solution by *Citrus limettioides* seed and its carbon derivative, Environ. Prog. Sustainable Energy, 34 (2015) 1384–1395.
[28] H. Abdulrazzaq, H. Jol, A. Husni, R. Abu-Bakr, Characterization and stabilisation of biochars obtained from empty fruit funch, wood, and rice husk, BioResources, 9 (2014) 2888–2898.
[29] N. Elboughdiri, The use of natural zeolite to remove heavy metals Cu(II), Pb(II) and Cd(II), from industrial wastewater, Cogent Eng., 7 (2020) 1782623, doi: 10.1080/23311916.2020.1782623.
[30] F. Ma, B. Zhao, J. Diao, Adsorption of cadmium by biochar produced from pyrolysis of corn stalk in aqueous solution, Water Sci. Technol., 74 (2016) 1335–1345.
[31] T.K. Sen, M. Mohammod, S. Maitra, B.K. Dutta, Removal of cadmium from aqueous solution using castor seed hull: a kinetic and equilibrium study, Clean – Soil Air Water, 38 (2010) 850–858.
[32] M. Mohammod, T.K. Sen, S. Maitra, B.K. Dutta, Removal of Zn^{2+} from aqueous solution using castor seed hull, Water Air Soil Pollut., 215 (2011) 609–620.
[33] K.G. Bhattacharyya, S.S. Gupta, Adsorptive accumulation of Cd(II), Co(II), Cu(II), Pb(II) and Ni(II) from water on montmorillonite: influence of acid activation, J. Colloid Interface Sci., 310 (2007) 411–424.
[34] J.N. Edokpayi, J.O. Odiyo, T.A.M. Msagati, E.O. Popoola, A novel approach for the removal of lead(II) ion from wastewater using mucilaginous leaves of *Diceriocaryum eriocarpum* plant, Sustainability, 7 (2015) 14026–14041.
[35] I.K. Rind, N. Memon, M.Y. Khuhawar, M.F. Lanjwani, Thermally activated mango peels hydrochar for fixed-bed continuous flow decontamination of Pb(II) ions from aqueous solution, Int. J. Environ. Sci. Technol., 19 (2022) 2835–2850.
[36] F.J. Alguacil, L. Alcaraz, I. García-Díaz, F.A. López, Removal of Pb^{2+} in wastewater via adsorption onto an activated carbon produced from winemaking waste, Metals, 8 (2018) 697, doi: 10.3390/met8090697.
[37] T.V. Tran, Q.T. Phuong Bui, T.D. Nguyen, N.T.H. Le, L.G. Bach, A comparative study on the removal efficiency of metal ions (Cu^{2+}, Ni^{2+}, and Pb^{2+}) using sugarcane bagasse-derived $ZnCl_2$-activated carbon by the response surface methodology, Adsorpt. Sci. Technol., 35 (2017) 72–85.
[38] W. Kim, R. Singh, Modified oyster waste shells as a value-added sorbent for lead removal from water, Bull. Environ. Contam. Toxicol., 108 (2022) 518–525.
[39] B.A. Ezeonuegbu, M.D. Abdulahi, C.M.Z. Whong, J.W. Sohunago, A. Athanasios, S.T. Elazab, Q. Naeem, C.A. Yaro, G.E.S. Batiha, Agricultural waste of sugarcane bagasse as efficient adsorbent for lead and nickel removal from untreated wastewater: biosorption, equilibrium isotherms, kinetics and desorption studies, Biotechnol. Rep., 30 (2021) e00614, doi: 10.1016/j.btre.2021.e00614.
[40] I. Lung, M. Stan, O. Opris, M.-L. Soran, M. Senila, M. Stefan, Removal of lead(II), cadmium(II), and arsenic(III) from aqueous solution using magnetite nanoparticles prepared by green synthesis with Box–Behnken design, Anal. Lett., 51 (2018) 2519–2531.
[41] H. Sultan, N. Ahmed, M. Mubashir, S. Danish, Chemical production of acidified activated carbon and its influences on soil fertility comparative to thermo-pyrolyzed biochar, Sci. Rep., 10 (2020) 595, doi: 10.1038/s41598-020-57535-4.
[42] G.A. Chávez-Prado, A.B. Benavides-García, L.A. Zambrano-Intriago, N.R. Maddela, L.S. Quiroz-Fernández, R.J. Baquerizo-Crespo, J.M. Rodríguez-Díaz, Novel application of tagua shell (*Phytelephas aequatorialis*) as adsorbent material for the removal of Pb(II) ions: kinetics, equilibrium, and thermodynamics of the process, Sustainability, 14 (2022) 1309, doi: 10.3390/su14031309.
[43] S.M. Beyan, T.A. Ambio, V.P. Sundramurthy, C. Gomadurai, A.A. Getahun, Adsorption phenomenon for removal of Pb(II) via Teff straw based activated carbon prepared by microwave-assisted pyrolysis: process modelling, statistical optimisation, isotherm, kinetics, and thermodynamic studies, Int. J. Environ. Anal. Chem., (2022), doi: 10.1080/03067319.2022.2026942.
[44] J. Acharya, J.N. Sahu, C.R. Mohanty, B.C. Meikap, Removal of lead(II) from wastewater by activated carbon developed from tamarind wood by zinc chloride activation, Chem. Eng. J., 149 (2009) 249–262.
[45] W.J. Weber, J.C. Morris, Kinetics of adsorption on carbon from solution, J. Sanit. Eng. Div. Am. Soc. Civ. Eng., 89 (1963) 31–60.
[46] A.K. Bhattacharya, C.J. Venkobachar, Removal of cadmium(II) by low cost adsorbents, J. Environ. Eng. Div.-ASCE, 110 (1984) 110–122.
[47] L.D. Michelson, P.G. Gideon, E.G. Pace, L.H. Kutal, US, Department of Industry, Office of Water Research and Technology, Bulletin No. 74, 1975.
[48] S. Malathi, R. Sudha, P. Anitha, P. Maheswari, M. Gomathi, K. Poornima, Removal efficiency of cadmium(II) from electroplating wastewater by chemically modified cottonseed cake carbon, Desal. Water Treat., 196 (2020) 377–387.